ICIC Express Letters
Volume **10**, Number **2**, February **2016**

 ISSN 1881-803X
pp. **433–438**

FOUR QUADRANT PMSM DRIVE SYSTEM VIA SINGLE NEURON ADAPTIVE CONTROL AND BACKSTEPPING

Mingling Shao, Haisheng Yu, Jinpeng Yu and Xiurong Chu

College of Automation Engineering
Qingdao University
No. 308, Ningxia Road, Qingdao 266071, P. R. China
yu.hs@163.com

Received July 2015; accepted September 2015

Abstract. *In the permanent magnet synchronous motor (PMSM) four quadrant system, for the purpose of getting the controllable direct current (DC)-bus voltage and unity power factor control, the single neuron direct model reference adaptive control (MRAC) controller is designed with new error function in the grid-side converter. Furthermore, to precisely achieve the speed tracking control in the motor-side converter, the controllers are studied according to the backstepping with unknown load torque by designing virtual control inputs and choosing appropriate Lyapunov functions. Finally, simulation results clearly exhibit that the controllers guarantee the good performance of the system.*
Keywords: Four quadrant, Permanent magnet synchronous motor, Single neuron direct model reference adaptive control, Backstepping

1. **Introduction.** The back-to-back converter with pulse width modulation (PWM) is a new technology in recent years to achieve four quadrant operation of the permanent magnet synchronous motor (PMSM) drive system [1]. For the grid-side converter and motor-side converter, there are still many deficiencies in conventional control strategies due to the variation of motor parameters, load disturbance and uncertainty effects [2,3]. Thus, the unity power factor control in the grid-side converter and the speed tracking control in the motor-side converter have become the key issues of the system. A direct grid current control strategy for LCL-filtered grid-connected inverters is proposed to mitigate the grid voltage disturbance [3]. A model-based direct power control (DPC) for three-phase power converters is designed to overcome problems that are associated with system parameter uncertainties in [4]. In [5], a robust nonlinear controller is synthesized using the damping function version of the backstepping design technique for the robust control of synchronous motor through AC/DC/AC converters. A robust control strategy based on sliding mode controller is proposed in [6], which allows the use of a small size direct current (DC)-link capacitor for the cascade of voltage controlled-rectifier/inverter-motor drive system.

In this paper, a new error function is adopted to design the single neuron direct model reference adaptive control (MRAC) controller in the grid-side converter [7]. Combining the derivation of reference model for PMSM in [8], the reference model of the grid-side converter is derived as first order system. To obtain the good speed tracking performance, the backstepping controllers are designed with unknown load torque in the motor-side [9]. At last, the simulation results clearly demonstrate the performance and feasibility of the proposed controllers.

The paper is organized as follows. Section 2 presents the control scheme and mathematical model of the system. Controller design of the grid-side converter is described in the Section 3. Section 4 presents the controller design of the motor-side converter. Moreover, the simulation results are given in Section 5. Section 6 states our conclusions.

2. **Control Scheme and Mathematical Model of the System.** The control scheme of the four quadrant PMSM drive system is viewed in Figure 1. In the grid-side converter, the single neuron direct MRAC controller is studied as the voltage controller to get the controllable DC-bus voltage and the unity power factor. The current controllers C_{gd} and C_{gq} are proportional integral (PI) controllers. In the motor-side converter, the backstepping controllers are adopted to improve the speed tracking performance.

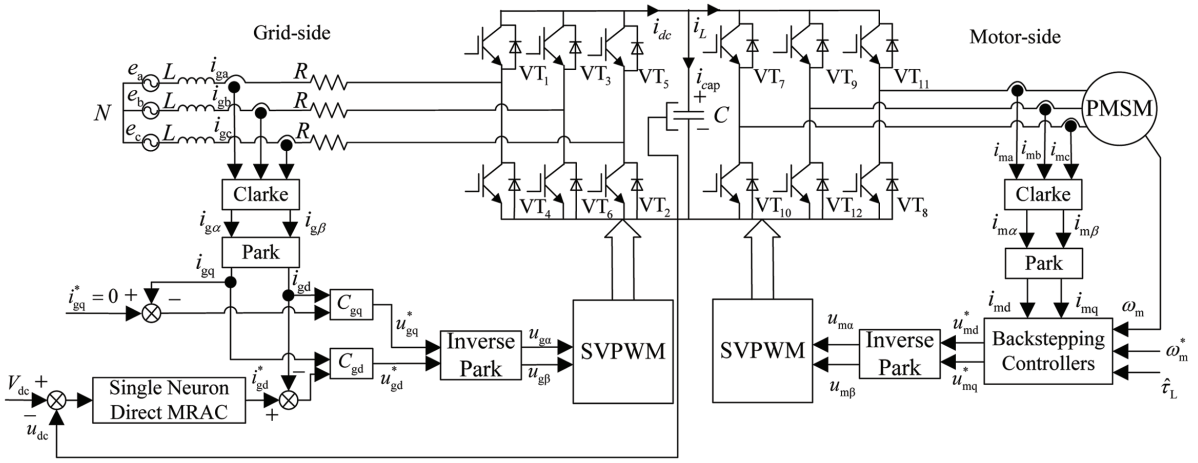

FIGURE 1. Control scheme diagram of the back-to-back four quadrant system

The mathematical model of the grid-side converter in a synchronously rotating dq reference frame can be expressed as [3]

$$\begin{cases} L\mathrm{d}i_{\mathrm{gd}}/\mathrm{d}t = e_{\mathrm{d}} - Ri_{\mathrm{gd}} + \omega_{\mathrm{g}} L i_{\mathrm{gq}} - v_{\mathrm{d}} \\ L\mathrm{d}i_{\mathrm{gq}}/\mathrm{d}t = e_{\mathrm{q}} - Ri_{\mathrm{gq}} - \omega_{\mathrm{g}} L i_{\mathrm{gd}} - v_{\mathrm{q}} \\ C\mathrm{d}u_{\mathrm{dc}}/\mathrm{d}t = \mu_{\mathrm{gd}} i_{\mathrm{gd}} + \mu_{\mathrm{gq}} i_{\mathrm{gq}} - i_{\mathrm{L}} \end{cases} \tag{1}$$

where ω_{g} denotes the angular frequency of the source voltage. The u_{dc} is the actual DC-bus voltage, μ_{gd} and μ_{gq} are the PWM duty ratio functions and $\mu_{\mathrm{gd}} = u_{\mathrm{gd}}/u_{\mathrm{dc}}$, $\mu_{\mathrm{gq}} = u_{\mathrm{gq}}/u_{\mathrm{dc}}$. The L is the grid-side filter inductance, R is the equivalent resistance, and C is the DC-link filter capacitor.

The mathematical model of PMSM in a synchronously rotating dq reference frame can be described by the following equations [10]

$$\begin{cases} L_{\mathrm{d}}\mathrm{d}i_{\mathrm{md}}/\mathrm{d}t = -R_{\mathrm{s}} i_{\mathrm{md}} + n_{\mathrm{p}}\omega_{\mathrm{m}} L_{\mathrm{q}} i_{\mathrm{mq}} + u_{\mathrm{md}} \\ L_{\mathrm{q}}\mathrm{d}i_{\mathrm{mq}}/\mathrm{d}t = -R_{\mathrm{s}} i_{\mathrm{mq}} - n_{\mathrm{p}}\omega_{\mathrm{m}} L_{\mathrm{d}} i_{\mathrm{d}} - n_{\mathrm{p}}\omega_{\mathrm{m}}\Phi + u_{\mathrm{qm}} \\ J\mathrm{d}\omega_{\mathrm{m}}/\mathrm{d}t = \tau - \tau_{\mathrm{L}} - B\omega_{\mathrm{m}} \end{cases} \tag{2}$$

$$\tau = n_{\mathrm{p}}\left[\left(L_{\mathrm{d}} - L_{\mathrm{q}}\right) i_{\mathrm{md}} i_{\mathrm{mq}} + \Phi i_{\mathrm{mq}}\right] \tag{3}$$

where R_{s} is the stator resistance, and Φ is the rotor flux linking the stator, respectively. The J is the moment of inertia, B is the friction coefficient, and n_{p} is the number of pole pairs, respectively. The ω_{m} is the mechanical angular speed. The τ and τ_{L} are electromagnetic torque and load torque, respectively.

3. **Controller Design of the Grid-Side Converter.** The single neuron direct MRAC controller is employed to get the i^*_{gd}, and PI control is adopted in the current controllers.

3.1. **Design of single neuron direct MRAC controller.** Assuming u_{dc}, $\dot{u}_{\mathrm{dc}}$, i_{gd} and i_{gq} are measurable signals, with $i^*_{\mathrm{gq}} = 0$ control, Equation (1) can be rewritten into $a_1\dot{u}_{\mathrm{dc}} + a_0 u_{\mathrm{dc}} = i_{\mathrm{gd}}$ with $a_1 = C/\mu_{\mathrm{gd}}$ and $a_0 = C/(R_{\mathrm{L}}\mu_{\mathrm{gd}})$. Thus, the reference model can be chosen as $b_1\dot{u}_{\mathrm{rdc}} + b_0 u_{\mathrm{rdc}} = V_{\mathrm{dc}}$. And $\boldsymbol{b} = (b_1, b_0)^{\mathrm{T}}$ is the parameters vector of reference

model. The u_{rdc} is the output of reference model and the V_{dc} is the given DC-bus voltage. Consequently, the transfer function can be gotten [8]

$$G_{\mathrm{g}}(s) = \frac{L\left[u_{\mathrm{rdc}}(t)\right]}{L\left[V_{\mathrm{dc}}(t)\right]} = \frac{U_{\mathrm{r}}(s)}{V(s)} = \frac{1}{b_1 s + b_0} \tag{4}$$

Thus, $u_{\mathrm{rdc}}(t) = (1/b_1)e^{-b_0 t/b_1} V_{\mathrm{dc}}$ can be obtained as the output of reference model.

As the large inertia link exists in the grid-side, thus $E_{\mathrm{g}} = \frac{1}{2}\left[(u_{\mathrm{rdc}} - u_{\mathrm{dc}}) + KD\left(\dot{u}_{\mathrm{rdc}} - \dot{u}_{\mathrm{dc}}\right)\right]^2$ is chosen as the new error function and KD is the variable differential coefficient. The ΔW and Δb of single neuron are gotten by gradient descent method. The system control structure is shown in Figure 2. The output of single neuron controller is $i^*_{\mathrm{gd}} = WV_{\mathrm{dc}} - b$, where W and b are weight and threshold of single neuron controller, respectively [7].

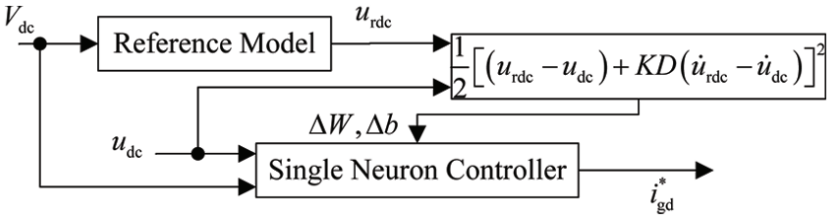

FIGURE 2. Simplified diagram of single neuron direct MRAC controller

The control target is that the error function $E_{\mathrm{g}} = e_{\mathrm{g}}^2/2$ tends to zero by adjusting the input weight and threshold. The control algorithm can be expressed as

$$\Delta W = -\eta_1 \frac{\partial E_{\mathrm{g}}}{\partial W} = e_{\mathrm{g}}(k)\eta_1 \frac{\partial e_{\mathrm{g}}}{\partial i^*_{\mathrm{gd}}} \frac{\partial i^*_{\mathrm{gd}}}{\partial W}, \quad \Delta b = -\eta_2 \frac{\partial E_{\mathrm{g}}}{\partial b} = e_{\mathrm{g}}(k)\eta_2 \frac{\partial e_{\mathrm{g}}}{\partial i^*_{\mathrm{gd}}} \frac{\partial i^*_{\mathrm{gd}}}{\partial b} \tag{5}$$

where η_1 and η_2 are learning rates of weight and threshold, respectively. The exact value of $\partial e_{\mathrm{g}}/\partial i^*_{\mathrm{gd}}$ cannot be gotten as the motor model is inaccurate. Thus, $\mathrm{sgn}(\partial e_{\mathrm{g}}/\partial i^*_{\mathrm{gd}})$ can be chosen to replace $\partial e_{\mathrm{g}}/\partial i^*_{\mathrm{gd}}$. Define $\delta = e_{\mathrm{g}}(k)$ and the control algorithm can be expressed as

$$\Delta W = \eta_1 \delta V_{\mathrm{dc}} \mathrm{sgn}(\partial e_{\mathrm{g}}/\partial i^*_{\mathrm{gd}}), \quad W(k+1) = W(k) + \Delta W \tag{6}$$

$$\Delta b = \eta_2 \delta V_{\mathrm{dc}} \mathrm{sgn}(\partial e_{\mathrm{g}}/\partial i^*_{\mathrm{gd}}), \quad b(k+1) = b(k) + \Delta b \tag{7}$$

3.2. **Design of current controllers.** The controller $\mathrm{C_{gq}}$ is studied as the q-axes current controller based on PI control and $i^*_{\mathrm{sq}} = 0$, and PI control is proposed for $\mathrm{C_{gd}}$ controller as the d-axes current controller.

$$u^*_{\mathrm{gd}} = \mathrm{K_{p1}}(i^*_{\mathrm{gd}} - i_{\mathrm{gd}}) + \mathrm{K_{i1}} \int_0^t (i^*_{\mathrm{gd}} - i_{\mathrm{gd}})\mathrm{d}t, \quad u^*_{\mathrm{gq}} = \mathrm{K_{p2}}(i^*_{\mathrm{gq}} - i_{\mathrm{gq}}) + \mathrm{K_{i2}} \int_0^t (i^*_{\mathrm{gq}} - i_{\mathrm{gq}})\mathrm{d}t \tag{8}$$

where $\mathrm{K_{p1}}$ is proportion coefficient and $\mathrm{K_{i1}}$ is integral coefficient of controller $\mathrm{C_{gd}}$, respectively. $\mathrm{K_{p2}}$ is proportion coefficient and $\mathrm{K_{i2}}$ is integral coefficient of controller $\mathrm{C_{gq}}$, respectively.

3.3. **System stability analysis.** Choose the Lyapunov function as $V_{\mathrm{g}}(k) = e_{\mathrm{g}}^2(k)/2$, which is positive definite. Thus

$$\Delta V_{\mathrm{g}}(k) = \frac{1}{2}e_{\mathrm{g}}^2(k+1) - \frac{1}{2}e_{\mathrm{g}}^2(k), \quad \Delta e_{\mathrm{g}}(k) = e_{\mathrm{g}}(k+1) - e_{\mathrm{g}}(k) \tag{9}$$

From Equation (5)

$$\Delta W = -\eta_1 \frac{\partial E_{\mathrm{g}}}{\partial e_{\mathrm{g}}} \frac{\partial e_{\mathrm{g}}}{\partial W} = -e_{\mathrm{g}}\eta_1 \frac{\partial e_{\mathrm{g}}}{\partial W}, \quad \Delta b = -\eta_2 \frac{\partial E_{\mathrm{g}}}{\partial e_{\mathrm{g}}} \frac{\partial e_{\mathrm{g}}}{\partial b} = -e_{\mathrm{g}}\eta_2 \frac{\partial e_{\mathrm{g}}}{\partial b} \tag{10}$$

According to $\Delta e_{\mathrm{g}}(k) = \Delta W \frac{\partial e_{\mathrm{g}}}{\partial W} + \Delta b \frac{\partial e_{\mathrm{g}}}{\partial b}$ and Equation (10)

$$\Delta e_{\mathrm{g}}(k) = -e_{\mathrm{g}} \left(\frac{\partial e_{\mathrm{g}}}{\partial W} \eta_1 \frac{\partial e_{\mathrm{g}}}{\partial W} + \frac{\partial e_{\mathrm{g}}}{\partial b} \eta_2 \frac{\partial e_{\mathrm{g}}}{\partial b} \right) = -e_{\mathrm{g}} \boldsymbol{p}^{\mathrm{T}} \boldsymbol{\eta} \boldsymbol{p} \tag{11}$$

where $\boldsymbol{\eta} = diag[\ \eta_1 \quad \eta_2\ ]$ and $\boldsymbol{p}^{\mathrm{T}} = [\ \partial e_{\mathrm{g}}/\partial W \quad \partial e_{\mathrm{g}}/\partial b\ ]$. Then $\Delta V_{\mathrm{g}}(k)$ can be rewritten as

$$\Delta V_{\mathrm{g}}(k) = \frac{1}{2} \left[-2 e_{\mathrm{g}} e_{\mathrm{g}} \boldsymbol{p}^{\mathrm{T}} \boldsymbol{\eta} \boldsymbol{p} + e_{\mathrm{g}} \boldsymbol{p}^{\mathrm{T}} \boldsymbol{\eta} \boldsymbol{p} e_{\mathrm{g}} \boldsymbol{p}^{\mathrm{T}} \boldsymbol{\eta} \boldsymbol{p} \right] = -\frac{1}{2} (e_{\mathrm{g}} \boldsymbol{p})^{\mathrm{T}} \left[2\boldsymbol{\eta} - \boldsymbol{\eta} \boldsymbol{p} \boldsymbol{p}^{\mathrm{T}} \boldsymbol{\eta} \right] (e_{\mathrm{g}} \boldsymbol{p}) \tag{12}$$

$\Delta V_{\mathrm{g}}(k)$ is negative definite with $0 < \boldsymbol{\eta} < 2(\boldsymbol{p}\boldsymbol{p}^{\mathrm{T}})^{-1}$. Applying Lyapunov stability theorem, the grid-side of the system is stable.

4. **Controller Design of the Motor-Side Converter.** The motor-side controllers are developed by backstepping with unknown load torque. According to the design of load torque observer in [10] and Equations (2) and (3), the following equations can be gotten

$$\begin{cases} \begin{bmatrix} \dot{\hat{\omega}}_{\mathrm{m}} \\ \dot{\hat{\tau}}_{\mathrm{L}} \end{bmatrix} = \begin{bmatrix} -B/J & -1/J \\ 0 & 0 \end{bmatrix} \begin{bmatrix} \hat{\omega}_{\mathrm{m}} \\ \hat{\tau}_{\mathrm{L}} \end{bmatrix} + \begin{bmatrix} 1/J \\ 0 \end{bmatrix} \tau + \begin{bmatrix} k_1 \\ k_2 \end{bmatrix} (y - \hat{y}) \\ \hat{y} = \begin{bmatrix} 1 & 0 \end{bmatrix} \begin{bmatrix} \hat{\omega}_{\mathrm{m}} & \hat{\tau}_{\mathrm{L}} \end{bmatrix}^{\mathrm{T}} \end{cases} \tag{13}$$

where $k_1 = -2a$ and $k_2 = a^2 J$, $\hat{\boldsymbol{x}} = \begin{bmatrix} \hat{\omega}_{\mathrm{m}} & \hat{\tau}_{\mathrm{L}} \end{bmatrix}^{\mathrm{T}}$ is the estimated state variable and $\boldsymbol{K} = \begin{bmatrix} k_1 & k_2 \end{bmatrix}^{\mathrm{T}}$ is the feedback gain matrix.

In this paper, the backstepping controllers are designed by the following steps.

Step 1: The speed tracking error can be defined as $e_{\omega_{\mathrm{m}}} = \omega_{\mathrm{m}}^* - \omega_{\mathrm{m}}$. Let $\hat{\tau}_{\mathrm{L}}$ be the estimated value of load torque τ_{L}, which is gotten by Equation (13). Using the Equations (2) and (3), the derivation of $e_{\omega_{\mathrm{m}}}$ can be described as

$$\dot{e}_{\omega_{\mathrm{m}}} = \dot{\omega}_{\mathrm{m}}^* - \dot{\omega}_{\mathrm{m}} = \dot{\omega}_{\mathrm{m}}^* + \hat{\tau}_{\mathrm{L}}/J + B\omega_{\mathrm{m}}/J - n_{\mathrm{p}} \left[(L_{\mathrm{d}} - L_{\mathrm{q}}) i_{\mathrm{md}} i_{\mathrm{mq}} + \Phi i_{\mathrm{mq}} \right]/J \tag{14}$$

The Lyapunov function is designed as $V_{\mathrm{m1}} = e_{\omega_{\mathrm{m}}}^2/2$. In order to obtain the stable feedback, substituting i_{mq}^* instead of i_{mq} into Equation (14), i_{mq}^* is selected as follows

$$i_{\mathrm{mq}}^* = J \left(\dot{\omega}_{\mathrm{m}}^* + \hat{\tau}_{\mathrm{L}}/J + B\omega_{\mathrm{m}}/J + k_3 e_{\omega_{\mathrm{m}}} \right)/n_{\mathrm{p}}\Phi \tag{15}$$

where k_3 is the feedback gain. Then $\dot{e}_{\omega_{\mathrm{m}}} = -k_3 e_{\omega_{\mathrm{m}}}$ and $\dot{V}_{\mathrm{m1}} = \dot{e}_{\omega_{\mathrm{m}}} e_{\omega_{\mathrm{m}}} = -k_3 e_{\omega_{\mathrm{m}}}^2 < 0$.

Step 2: Let $e_{\mathrm{mq}} = i_{\mathrm{mq}}^* - i_{\mathrm{mq}}$ be the q-axes current error, and then the derivation of e_{mq} is derived as

$$\dot{e}_{\mathrm{mq}} = \dot{i}_{\mathrm{mq}}^* - \left(-R_{\mathrm{s}} i_{\mathrm{mq}}/L_{\mathrm{q}} - n_{\mathrm{p}} \omega_{\mathrm{m}} i_{\mathrm{md}} L_{\mathrm{d}}/L_{\mathrm{q}} - n_{\mathrm{p}} \omega_{\mathrm{m}} \Phi/L_{\mathrm{q}} + u_{\mathrm{mq}}/L_{\mathrm{q}} \right) \tag{16}$$

A new Lyapunov function is chosen as $V_{\mathrm{m2}} = V_{\mathrm{m1}} + e_{\mathrm{mq}}^2/2$. In order to obtain the stable feedback, u_{mq} can be set as follows

$$u_{\mathrm{mq}} = \dot{i}_{\mathrm{mq}}^* L_{\mathrm{q}} + L_{\mathrm{q}} k_4 e_{\mathrm{mq}} + R_{\mathrm{s}} i_{\mathrm{mq}} + n_{\mathrm{p}} \omega_{\mathrm{m}} L_{\mathrm{d}} i_{\mathrm{md}} + n_{\mathrm{p}} \omega_{\mathrm{m}} \Phi \tag{17}$$

where k_4 is the feedback gain. Substituting Equation (17) into Equation (16) can have $\dot{e}_{\mathrm{mq}} = -k_4 e_{\mathrm{mq}}$, then $\dot{V}_{\mathrm{m2}} = \dot{V}_{\mathrm{m1}} + e_{\mathrm{mq}} \dot{e}_{\mathrm{mq}} = \dot{V}_{\mathrm{m1}} - k_4 e_{\mathrm{mq}}^2 < 0$.

Step 3: Let $e_{\mathrm{md}} = i_{\mathrm{md}}^* - i_{\mathrm{md}}$ be the d-axes current error, and then the derivation of e_{md} is written as

$$\dot{e}_{\mathrm{md}} = \dot{i}_{\mathrm{md}}^* - \dot{i}_{\mathrm{md}} = \dot{i}_{\mathrm{md}}^* + R_{\mathrm{s}} i_{\mathrm{md}}/L_{\mathrm{d}} - n_{\mathrm{p}} \omega_{\mathrm{m}} i_{\mathrm{mq}} L_{\mathrm{q}}/L_{\mathrm{d}} - u_{\mathrm{md}}/L_{\mathrm{d}} \tag{18}$$

A new Lyapunov function is constructed as $V_{\mathrm{m3}} = V_{\mathrm{m2}} + e_{\mathrm{md}}^2/2$. In order to obtain the stable feedback, u_{md} is defined as

$$u_{\mathrm{md}} = L_{\mathrm{d}} \dot{i}_{\mathrm{md}}^* + R_{\mathrm{s}} i_{\mathrm{md}} - n_{\mathrm{p}} \omega_{\mathrm{m}} L_{\mathrm{q}} i_{\mathrm{mq}} + L_{\mathrm{d}} k_5 e_{\mathrm{md}} \tag{19}$$

where k_5 is the feedback gain. Substituting Equation (19) into Equation (18) can have $\dot{e}_{\mathrm{md}} = -k_5 e_{\mathrm{md}}$, then $\dot{V}_{\mathrm{m3}} = \dot{V}_{\mathrm{m2}} + e_{\mathrm{md}} \dot{e}_{\mathrm{md}} = \dot{V}_{\mathrm{m2}} - k_5 e_{\mathrm{md}}^2 < 0$.

Let $V_{\mathrm{m4}} = \left(e_{\omega_{\mathrm{m}}}^2 + e_{\mathrm{mq}}^2 + e_{\mathrm{md}}^2\right)/2 > 0$, and then $\dot{V}_{\mathrm{m4}} = -k_3 e_{\omega_{\mathrm{m}}}^2 - k_4 e_{\mathrm{mq}}^2 - k_5 e_{\mathrm{md}}^2 < 0$ can be obtained. Thus, according to the Lyapunov stability theorem, the motor-side of the system is stable.

5. **Simulation Results.** To assess the feasibility of the proposed control scheme, the performance of the proposed controllers is carried out by MATLAB/Simulink under the conditions as follows. The grid-side parameters: $\omega_{\mathrm{g}} = 50\mathrm{Hz}$, $R = 1\Omega$, $L = 15\mathrm{mH}$, $C = 2200\mu\mathrm{F}$, $KD = 0.025$, $\eta_1 = 0.001$, $\eta_2 = 0.001$, $W(0) = 0.5$, $b(0) = 0.1$. The motor-side parameters: $R_{\mathrm{s}} = 2.875\Omega$, $n_{\mathrm{p}} = 4$, $L_{\mathrm{d}} = L_{\mathrm{q}} = 8.5\mathrm{mH}$, $J = 0.035\mathrm{kg}\cdot\mathrm{m}^2$, $\Phi = 0.175\mathrm{Wb}$, $B = 0.0001\mathrm{N}\cdot\mathrm{m}\cdot\mathrm{s}$, $a = 500$.

The given DC-bus voltage is $V_{\mathrm{dc}} = 300\mathrm{V}$ and the time of simulations is $t = 1.0\mathrm{s}$, and at $0.2 \sim 0.4\mathrm{s}$, ω_{m}^* is $400\mathrm{r/min}$ and τ_{L} is $2\mathrm{N}\cdot\mathrm{m}$. At $0.4 \sim 0.6\mathrm{s}$, ω_{m}^* is $0\mathrm{r/min}$ and τ_{L} is $-2\mathrm{N}\cdot\mathrm{m}$. At $0.6 \sim 0.8\mathrm{s}$, ω_{m}^* is $-400\mathrm{r/min}$ and τ_{L} is $-5\mathrm{N}\cdot\mathrm{m}$. At $0.8 \sim 1.0\mathrm{s}$, ω_{m}^* is $0\mathrm{r/min}$ and τ_{L} is $5\mathrm{N}\cdot\mathrm{m}$. The simulation curves of the system are shown in Figures 3-6.

Figure 3 denotes the speed curve of motor-side, which demonstrates that the system has good speed tracking performance. In Figure 4, the dotted line represents the observed load torque curve with load observer and the solid line represents the given load torque curve. It is shown that the load torque observer can observe the load torque precisely.

In Figure 5, the dotted line represents the given DC-bus voltage curve and the solid line represents the actual DC-bus voltage curve. It is shown that the DC-bus voltage is controllable. In Figure 6, the dotted line represents the q-axes current curve i_{gq} and the solid line represents the d-axes current curve i_{gd}. As can be seen from Figures 5 and 6, the DC-bus voltage is subjected to fluctuation during the motor electric and braking process. That is, the DC-bus voltage will be lower than the reference value when the motor is in the electric process. And the DC-bus voltage will be higher than the reference value when the motor is in the braking process. However, the DC-bus voltage can quickly restore to the stable state under the proposed method when the motor is in the steady state.

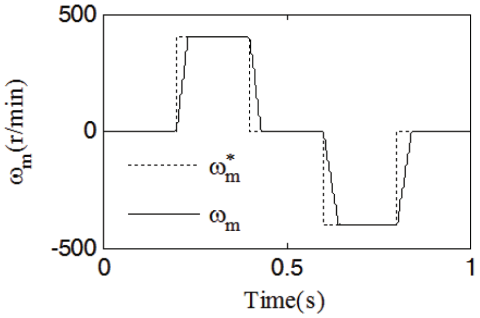

FIGURE 3. Speed curve in motor-side

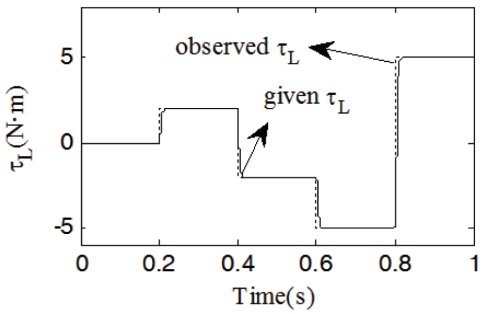

FIGURE 4. Load torque curve in motor-side

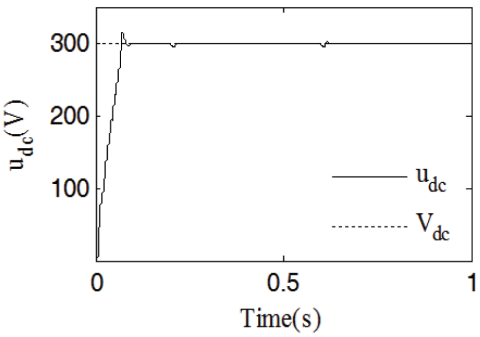

FIGURE 5. DC-bus voltage curve in grid-side

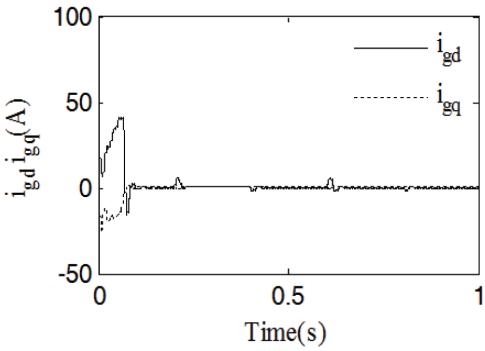

FIGURE 6. Current curve in grid-side

6. **Conclusions.** In this paper, for the purpose of getting the unity power factor in the four quadrant PMSM drive system, the single neuron direct MRAC controller with new error function is adopted in the grid-side. In order to improve the speed tracking ability, the motor-side controller is designed via the backstepping method. Thus, the system can not only achieve the unity power factor control, but also can have good dynamic and steady state performances. At last, the simulation results illustrate that the system can achieve the bidirectional flow of energy and the PMSM can realize the smooth operating in the four quadrant via the natural transition between the motor electric state and the braking state. In the future research, the proposed control scheme will be realized by DSP2812.

Acknowledgement. This work is supported by the National Natural Science Foundation of China (61573203, 61573204).

REFERENCES

[1] L. He, J. Xiong, H. Ouyang, P. Zhang and K. Zhang, High-performance indirect current control scheme for railway traction four-quadrant converters, *IEEE Trans. Industrial Electronics*, vol.61, no.12, pp.6645-6654, 2014.

[2] B. G. Gu and K. Nam, A DC-link capacitor minimization method through direct capacitor current control, *IEEE Trans. Industry Applications*, vol.42, no.2, pp.573-581, 2006.

[3] Y. Jia, J. Zhao and X. Fu, Direct grid current control of LCL-filtered grid-connected inverter mitigating grid voltage disturbance, *IEEE Trans. Power Electronics*, vol.29, no.3, pp.1532-1541, 2014.

[4] S. Vazquez, J. A. Sanchez, J. M. Carrasco, J. I. Leon and E. Galvan, A model-based direct power control for three-phase power converters, *IEEE Trans. Industrial Electronics*, vol.55, no.4, pp.1647-1657, 2008.

[5] A. El Magri, F. Giri, A. Abouloifa and F. Z. Chaoui, Robust control of synchronous motor through AC/DC/AC converters, *Control Engineering Practice*, vol.18, pp.540-553, 2010.

[6] P. Liutanakul, S. Pierfederici and F. Meibody-Tabar, Nonlinear control techniques of a controllable rectifier/inverter-motor drive system with a small dc-link capacitor, *Energy Conversion and Management*, vol.49, pp.3541-3549, 2008.

[7] H. Yu, J. Yu, N. Zhu and Q. Wei, Speed regulation of permanent magnet synchronous motor based on neuron adaptive control, *ICIC Express Letters, Part B: Applications*, vol.4, no.3, pp.565-571, 2013.

[8] C. Gao, Y. Shen and Z. Ji, Model reference fuzzy adaptive control of permanent magnet synchronous motor, *Journal of System Simulation*, vol.20, no.7, pp.1817-1820, 2008.

[9] M. Karabacak and H. I. Eskikurt, Design, modelling and simulation of a new nonlinear and full adaptive backstepping speed tracking controller for uncertain PMSM, *Applied Mathematical Modelling*, vol.36, pp.5199-5213, 2012.

[10] H. Yu, J. Yu and Y. Wang, Energy-shaping control of PMSM based on maximum output power and load torque observer, *ICIC Express Letters*, vol.7, no.1, pp.241-246, 2013.